PNAS RESEARCH ARTICLE | IMMUNOLOGY AND INFLAMMATION

Dynamics and variegation in the Treg response to Interleukin-2

Kumba Seddu[a,b], Kaitavjeet Chowdhary[a], Molly Henderson[a], Jakub Tomala[c], Odhran Casey[a], Yi Cao[a], Diane Mathis[a], Jamie B. Spangler[b,c,d], and Christophe Benoist[a,1]

Contributed by Christophe Benoist; received July 25, 2025; accepted October 21, 2025; reviewed by Leslie J. Berg, Alexander Y. Rudensky, and Tadatsugu Taniguchi

Interleukin-2 (IL2) is the key trophic factor for T regulatory (Treg) cells, controlling their differentiation and homeostasis. To understand how temporally regulated responses to IL2 unfold in Tregs, we performed fine time-course analyses, at population and single-cell levels, of changes in chromatin architecture and mRNAs induced by IL2 in Tregs in vivo. The data revealed responses that were largely uniform in rTreg, but diverse among aTregs, matching different STAT5 signal transduction efficiency. Individual Tregs displayed divergences in the preponderance of changes that may be attributed to STAT1 or STAT5 signal transduction downstream of IL2. Chromatin analysis identified an evolving implication of transcription factors that accounted for the waves of responsive genes. Covalent cytokine/Ab complexes that preferentially trigger high- (heterotrimer) or low-affinity (heterodimer) IL2 receptors activated the same signatures, yet with strong quantitative variations, especially in NK cells. Thus, IL2 is not a monolithic activator for Tregs, but a variegated sculptor of Treg identity.

cytokines | immune response | Treg cells

Significance

Interleukin-2 (IL2) is essential for Treg cell maintenance, but how its effects on Treg cells unfold, and whether Treg cells are heterogenous in their responses to IL2, are poorly understood. By analyzing mRNA and chromatin responses to IL2 in Tregs over time and at single-cell resolution, we reveal distinct signaling dynamics and transcriptional trajectories, in part shaped by differential STAT pathway usage. The lower responses observed in previously activated aTreg subsets, relative to rTregs, may inform the interpretation of clinical trials involving IL2 to modulate Tregs, as the expanded populations may not be the most useful ones.

Interleukin-2 (IL2) is a regulator of T cell biology, orchestrating immune responses through its effects on various immune cell subsets (1–3). While IL2 was initially recognized for its ability to expand activated T cells (4, 5), an even more important aspect of its role on immune homeostasis was recognized to stem from its impact on regulatory T cells (Tregs) (6, 7). Tregs, characterized by the transcription factor FoxP3, play a central and nonredundant role in the ordered operation of the immune system in many contexts: tolerance to self vs. autoimmune deviation, feto-maternal tolerance, allergy, responses to infections (8), with additional functions in tissue homeostasis and repair in less specifically immunological contexts (9). Although Tregs in lymphoid organs have been shown to comprise several distinct "poles", the most general of these distinctions is the difference between "resting" (rTreg, occasionally "cTreg") and "activated" (aTreg or eTreg) (10–14). rTreg tend to dominate in lymphoid organs, and aTregs in tissues, but this bias is only partial. aTreg and rTreg have distinct transcriptomes and chromatin organization (15–17).

IL2 is produced by activated conventional T cells (Tconv), but not at all by Tregs, which enables feedback loops that tune Treg numbers to the activation intensity of the Tconv cells they regulate (6). IL2 controls many aspects of Treg biology from differentiation in the thymus (18, 19) to homeostatic control in the periphery (20). Recent work shows the existence of microdomains in lymphoid organs, in which activated IL2-producing Tconv recruit a circle of Tregs, which in turn limits Tconv clonal expansion and leads to pruning of the Tconv repertoire (21, 22).

Given their critical role in immune regulation, Tregs have become prime therapeutic targets for a number of diseases, and many approaches aim to manipulate Tregs through IL2 (23). The therapeutic potential of IL2 has been hindered by its pleiotropic activation of natural killer (NK) and effector T cells along with Tregs. This translational challenge has motivated the engineering of IL2 variants (24) with selectivity for the high-affinity heterotrimeric IL2 receptor, composed of IL2Rα (CD25 (encoded by *Il2ra*), IL-2Rβ (CD122 encoded by *Il2rb*) and the signaling common γ-chain (γc, CD132, encoded by *Il2rg*). This high-affinity (KD~10 pM) IL2 receptor is preferentially expressed on Tregs, whereas the lower-intermediate-affinity (KD~1 nM) dimeric IL2 receptor (composed of only CD122 and CD132) is expressed on NK cells and activated effector T cells. Thus, IL2-based molecules engineered to preferentially bind the heterotrimeric IL2 receptor" should selectively expand Treg cells while minimizing activation of NK and effector T cells.

IL2 signals primarily through activation of JAK1/3 kinases and phosphorylation of STAT5 (1), which then shuttle to the nucleus and directly activates transcription [for instance, in its role as a Treg regulator, stabilizing FoxP3 expression by binding the *CNS2* enhancer in the *Foxp3* locus (25)]. But IL2 also activates other STAT family members (26) and several other signaling pathways (1, 3). This breadth of IL2 signaling pathways

Author affiliations: [a]Department of Immunology, Harvard Medical School, Boston, MA 02115; [b]Department of Molecular Microbiology and Immunology, Johns Hopkins Bloomberg School of Public Health, Baltimore, MD 21205; [c]Department of Chemical and Biomolecular Engineering, Johns Hopkins University, Baltimore, MD 21218; and [d]Department of Biomedical Engineering, Johns Hopkins University School of Medicine, Baltimore, MD 21218

Author contributions: K.S. and C.B. designed research; K.S., K.C., M.H., and Y.C. performed research; J.T. and J.B.S. contributed new reagents/analytic tools; K.S., K.C., M.H., O.C., and Y.C. analyzed data; D.M. and C.B. supervised research; and K.S., D.M., J.B.S., and C.B. wrote the paper.

Reviewers: L.J.B., University of Colorado-Anschutz Medical Campus; A.Y.R., Memorial Sloan Kettering Cancer Center; and T.T., The University of Tokyo.

The authors declare no competing interest.

[1]To whom correspondence may be addressed. Email: cbdm@hms.harvard.edu.

This article contains supporting information online at https://www.pnas.org/lookup/suppl/doi:10.1073/pnas.2518991122/-/DCSupplemental.

Published November 20, 2025.

was most dramatically shown by a phosphoproteomic analysis which revealed hundreds of changes in IL2 treated T cells (27). The best recognized IL2-responsive pathways include the SHC>Ras>Erk cascade (28), and the metabolism-controlling PI3K>AKT>mTOR pathway (29, 30).

A few recent studies have shown a strong impact of IL2 on chromatin accessibility and transcription (31–34). Many of these effects were shared with other cytokines that signal through the "common γ chain," or were elicited by other cytokines in different cells (31). IL2 signature transcripts also overlapped with responses induced by Interferons and proinflammatory cytokines (35). Correspondingly, IL2 induced shifts in chromatin accessibility in Treg genomes over time, particularly at open chromatin regions (OCRs) enriched in binding sites for STAT5 or NF-κB (32).

In this study, we combine population and single-cell analyses of chromatin remodeling and transcriptional changes in Tregs in response to IL2 over time. We define temporally coherent gene sets and their responsiveness to signaling via high- or intermediate-affinity receptors, then ask how the temporally regulated responses to IL2 unfold at the single-Treg level: are responses homogenous and synchronous in all cells, or do different clusters of cells preferentially activate particular gene modules? Indeed, we identify several levels of heterogeneity, particularly marked among aTreg populations, and some disconnect between response signatures that may be downstream of STAT1 or TAT5 activation. We build on our previous machine learning of the Treg regulatory network (17), project IL2 induced changes into that framework, and connect to the different TFs that dynamically control the unfolding of the response. This work deepens our understanding of IL2-controlled Treg biology, with significant implications for fine-tuning IL2-based immunotherapies.

Results

The Evolution of Transcriptomic Responses to IL2 in Tregs Over Time. As a preliminary to the main single-cell studies, we applied population RNAseq on finely sorted Treg cells. Although population RNAseq lacks the ability to parse groups of cells with different response profiles, it yields deeper and more robust DEG (differentially expressed genes) signatures. Our prior study (31) used IL2 complexed with the IL2 monoclonal antibody JES6, which stabilizes IL2 (which otherwise has a very short half-life in vivo) and favors activation through CD25 and the high-affinity IL2 receptor trimer (36). In our previous work, a cytokine/mAb dose of 10ug IL2/100ug JES6 was administered i.v. (31) To ensure the present experiments were performed with full exposure to IL2 and to avoid confounding effects from competition for limiting cytokine, we first performed a dose/response analysis, ranging from cytokine/mAb dose of 0.1/1 to 10/100 μg sorting splenic Treg cells 2 h later. As illustrated in *SI Appendix*, Fig. S1, the vast majority of genes responded largely in sync, reaching full response around the 1 μg dose. Only a few genes deviated from this general response profile, either requiring a higher dose (interestingly including the proapoptotic gene *Bax*). To ensure saturation, the 10 μg dose was used in most subsequent experiments.

To obtain robust time-resolved signatures of IL2 in Tregs, we performed a time-course analysis of the response to IL2/JES6 complexes *in vivo,* ranging from 1 to 128 h. In keeping with ref. 32, we observed an evolution of the response over time, not as an amplification but with clear temporal transitions in the inductive response relative to PBS-treated controls (Fig. 1 *A* and *B* and Dataset S1). Three main sets of genes could be identified. Induction of Early responder genes was clear by 2 h (including a small subset fully activated by 1 h, *Osm*, *Lta, Il2ra*) and peaked by 4 h, with a gradual decline thereafter. A "Mid-late" set did not show activation until 8 or 16 h after IL2 and peaked by 64 h. Finally, a "Late" set was only induced at 64 to 128 h. As previously reported, the component of genes repressed by IL2 was again substantial. It also showed a temporal trend, albeit more diffuse, as most of the transcripts underexpressed at 2 or 4 h were still down at 64 or 128 h relative to controls (Fig. 1*A*). These successive waves of induction resulted in a response that varied over time, but remained comparatively stable in terms of the magnitude of changes. The early response included many of the typical IL2 responsive genes such as *Il2ra, Myc, Lif, Cish*, and encompassed several of the profound rearrangements in cellular functions that have been described, including many Myc and mTOR targets (31, 32).

Comparative Analysis of Signals Delivered Via CD25 and CD122. Treg cells prototypically depend on the high-affinity IL2 receptor α/β/γtrimer to receive signals from IL2, but they also express the intermediate-affinity β/γ dimer. Although the trimeric receptor would be expected to account for most of the signaling and transcriptional effects in Tregs, because of its 100-fold higher

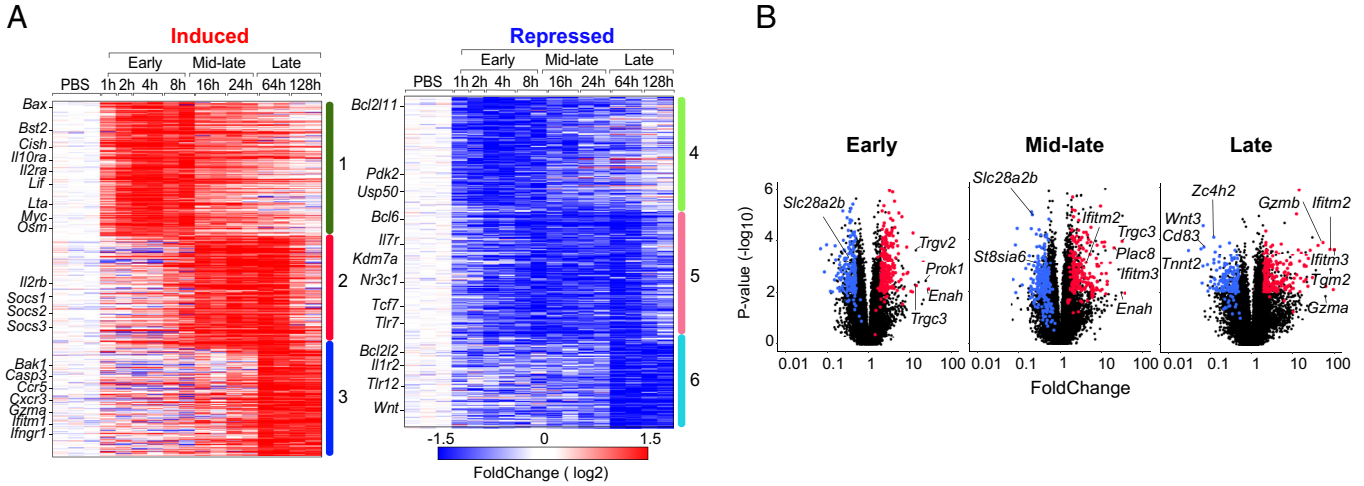

Fig. 1. Time-course of transcriptomic responses to IL2 in Tregs. (*A*) *Foxp3*$^{IRES\text{-}GFP}$/B6 mice were stimulated systemically with mouse IL2/JES6 complexes and splenic Tregs were sorted at the indicated timepoints for profiling by population RNASeq. An overview of the 1,288 upregulated and downregulated genes (FC>2 or <0.5, PV<0.01 between controls and groups of times) post stimulation cluster into three main gene sets, early, mid-late, and late timepoint. (*B*) Volcano plots of 4, 16, and 64 h IL2/JES6-treated vs. PBS control representing early, mid-late, and late timepoint with corresponding overlaid induced (red) and repressed (blue) gene signatures highlighted that meet FoldChange >2 or 0.5 with a *P* value < 0.01.

affinity, it was possible that the two receptors might account for different segments of the Treg response to IL2. To address this question, we used two "immunocytokines," (IC) that link IL2 to anti-IL2 antibodies that bias its receptor-binding. Compared to IL2/antibody complexes, ICs enforce a stable interaction between the cytokine and antibody, while also imposing a stoichiometrically matched 2:1 cytokine:antibody ratio (37–39). Specifically, we used F5111 IC, which preferentially activates the heterotrimeric α/β/γ receptor (39), and F10 IC which activates the β/γ dimer (37, 38). Splenic Tregs and NK cells were sorted 4 h later for population profiling—including NK cells as a specificity control, as they are expected to signal quasi-exclusively through the heterodimeric IL2 receptor. There was a stark and symmetrical difference in the responses to the two ICs in Treg and NK cells (Fig. 2*A* and Dataset S2). At arbitrary FoldChange = 2 (FC) and *t* test *P*.value = 0.01 thresholds, 132 genes were induced by F5111 in Tregs, but only 1 by F10. Conversely, zero genes scored as induced by F5111 in NK cells, but 40 by F10. These quasi-exclusive effects fit with the differential relevance of trimeric and dimeric receptors in Treg and NK cells. On the other hand, a more nuanced conclusion was apparent in the FC/FC plots of Fig. 2*B*, which compared directly the effects of F5111 and F10 in the two cell-types. Clearly, both ICs induce the same responses in Tregs, but more strongly for F5111 as reflected by the off-diagonal distribution (globally amounting to a two- threefold difference in activity). NK cells also showed strong overlap between the two IC, here with a much stronger advantage for the dimer-biased IC. These results showed that there is a quantitative but no qualitative difference between responses elicited by heterotrimeric vs. heterodimeric IL2 receptor complex engagement in Tregs, with no gene modules specifically induced by one or the other (consistent with the fact that both receptors employ the same β and γ signaling subunits). From a practical or therapeutic standpoint, one should expect that next-generation compounds aimed at NK or CD8+ T cells may also have nonnegligible effects in Tregs.

The Treg Transcriptomic Responses to IL2 in Single-Cells. With these robust signatures in hand, we then proceeded with our main goal, to parse at the single-cell level the evolution of Treg responses to IL2. Do all Tregs respond similarly to IL2, are some clusters more or less responsive, and are different gene modules activated in different groups of cells, all distinctions that would be masked by the averaging of population profiling. As for Fig. 1, Foxp3-GFP reporter mice were treated with mIL2/JES6 complexes (10 μg IL2/100 μg JES6), and GFP+ splenic Tregs were purified by flow cytometry at different times, and profiled by single-cell RNAseq (two mice at each time point), Importantly, the entire experiment was multiplexed by hashtagging into the same run (40), which ensures ideal comparability between samples. A UMAP projection (Uniform Manifold Approximation and Projection) of the entire dataset is displayed in Fig. 3*A*. In the starting population, all clusters were positive for *Il2ra*, confirming that all were Treg cells, and rTreg and aTreg cells were distinguished with the usual signatures (17), consistent with the expression of the Tcf7 TF.

Within this framework, the distribution of cells from control mice was stable (Fig. 3 *B*, *Left*) but a cell trajectory unfolded over time after IL2 treatment. Most clearly, the cloud of rTreg cells shifted leftward, apparently synchronously during the first few hours (curved arrow). In contrast, cells in the aTreg section showed less dramatic changes at these early times (arrowhead). Beyond 8 h, the counterclockwise evolution continued, including transition through the leftmost area (clusters 9 and 10 of Fig. 1*A*, which

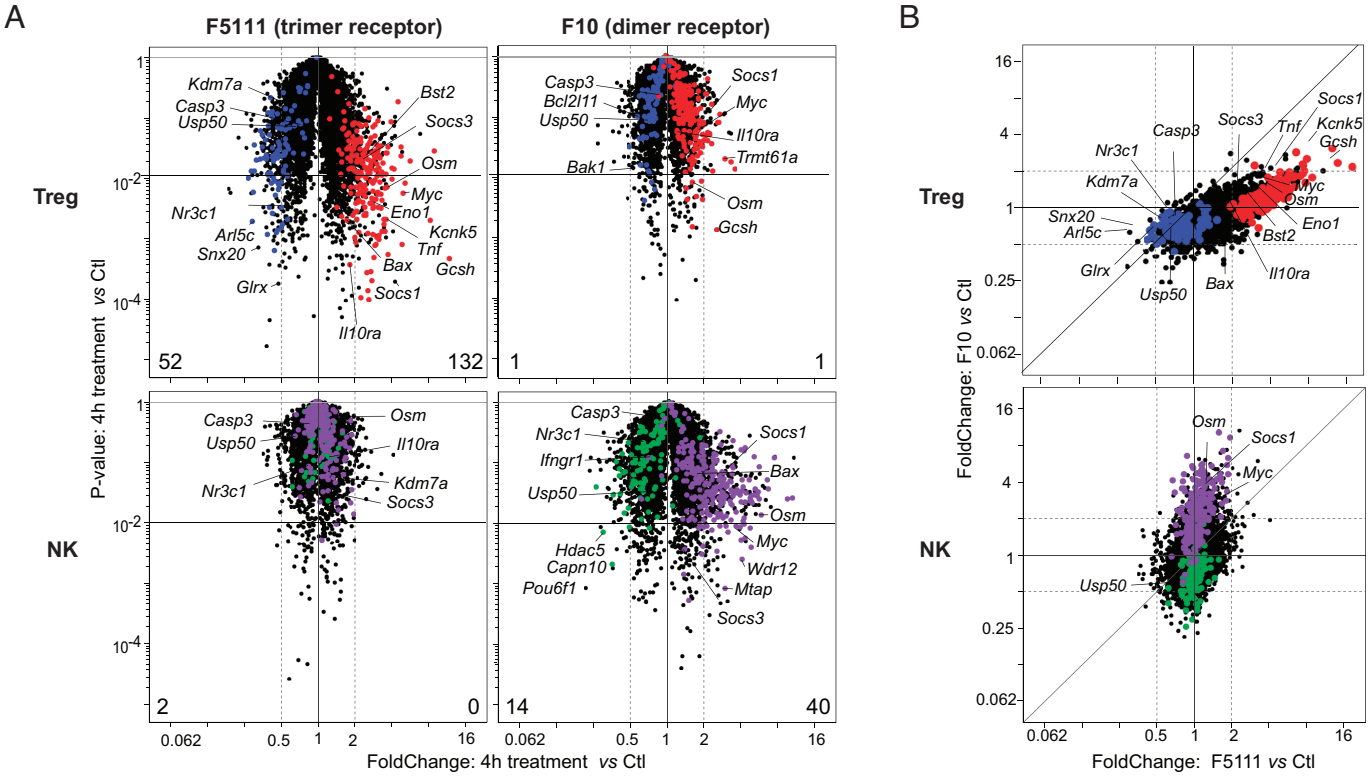

Fig. 2. Comparative transcriptomic responses to IL2 via dimeric or trimeric receptors. (*A*) Paired volcano plots comparing responses to F5111- (trimeric receptor bias) and F10-treated (dimeric receptor bias) vs. PBS controls in Tregs and NK cells at 4 h post stimulation. The early induced (red) and repressed (blue) gene sets from Fig. 1*A* are highlighted in Tregs; genes induced (purple) and repressed (green) in NK cells (from ref. 31) are highlighted in NK cells. Numbers at the bottom of each panel are the numbers of genes with FoldChange >2 or <0.5, with a Welsh's *t* test value <0.01. (*B*) FoldChange/FoldChange plots comparing responses to F5111 IC (x-axis) and F10 IC (y-axis) in Tregs (*Top*) and NK cells (*Bottom*). Induced and repressed gene sets are highlighted as in *A*.

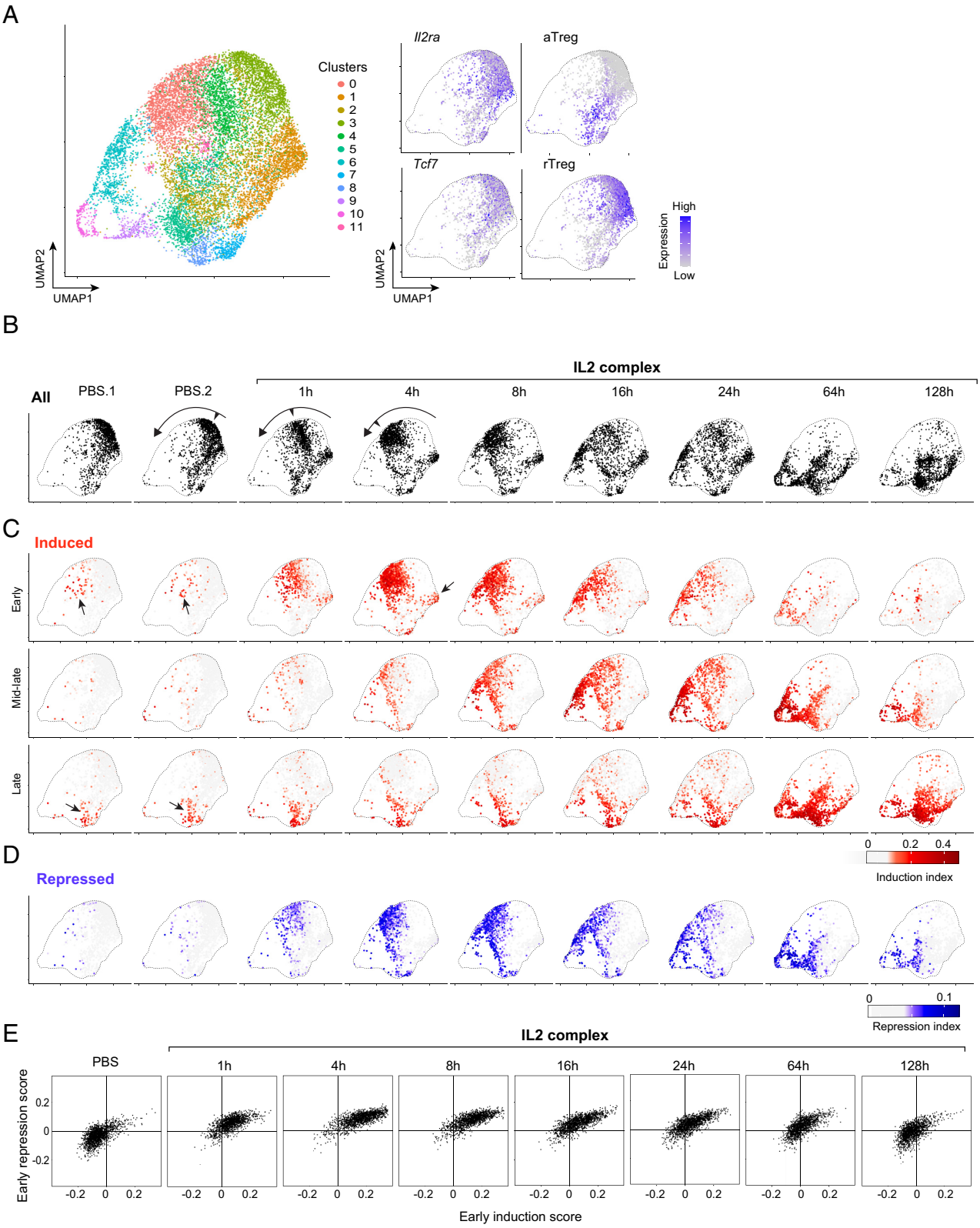

Fig. 3. The transcriptomic responses to IL2 in Tregs reveals heterogeneity and homogeneity at the single cell level. As for Fig. 1, FoxP3 reporter mice were treated with IL2/JES6 complexes and spleen Treg cells sorted after different times for scRNAseq. (*A*) UMAP in the scRNASeq space of all cells (all timepoints combined), colored according to Louvain clustering. For orientation, expression in PBS control samples of key Treg genes (*Il2ra, Tcf7*) and states (aTreg, rTregs) are visualized at right. (*B*) Position of cells at each timepoint (replicates pooled) projected onto the UMAP of *A*; curved arrows highlight the trajectory of rTreg cells. (*C*) As *B*, each cell color-coded according to expression of the IL2-induced signature genes (early, mid or late, from Fig. 1*A*, listed in Dataset S3). Cells with high IL2-induction score in the controls are indicated with arrows, as is a "nub" of rTregs cells with comparatively low responses (see also Fig. 5*B*). (*D*) As *C*, for the combined IL2-repressed signature. (*E*) Early induction and repression scores were calculated for each cell based on the signatures from Fig. 1*A*, and shown on a scatter plot (each dot is a cell at a given timepoint).

corresponds to cycling cells, see below). All cells at 128 h finally settled in the aTreg zone of the UMAP.

Changes in the position of a cell cloud on a UMAP denote changes in gene expression, but it was important to relate these to the IL2-induced signatures described above. From the temporal signature genesets defined in Fig. 1*A*, we computed induction scores for each of these signatures (Fig. 3 *C* and *D*). The three induction scores generally followed the expected time course, with strongest scores in different portions of the time-resolved UMAP. Clearly, the early shift of rTregs (curved arrow) corresponded to the appearance of the early signature (Fig. 3*C*). Close examination revealed that the induction of the signatures was not uniform across all cells. For instance, cells in the aTreg zone at 1 and 4 h showed much less of the early signature than those in the rTreg zone (a point further analyzed below). Similarly, cells in the extreme right nub of the UMAP (cluster 2 of Fig. 3*A*) had a lower mid-late signature score than the rest of the rTregs at the 4 to 16 h timepoints. In contrast to these inductive events that seem to vary between groups of cells, an index computed from the genes repressed by IL2 appeared more uniformly distributed; note, for example, how the group of aTreg cells that had low induction score at 1 or 4 h showed a robust repression score (Fig. 3*D*).

To better appreciate the heterogeneity in Treg cells responding to IL2, we plot in Fig. 3*E* the early induction and repression scores for every cell, computed as above. Overall, there were no striking outlier groups of cells. As predicted from the graphic representation on the UMAP plots of Fig. 3*D*, the repression score (Y-axis in Fig. 3*E*) rose very quickly and quite uniformly in all cells (essentially set by 1 h, with little variation). In contrast, there was much more spread in the induction score.

We also noted that a fraction of the splenic Tregs in untreated mice exhibited signs of stimulation by IL2 (arrows in Fig. 3*C*). These rare (~5%) cells were displaced from the main group of rTreg or aTreg in the UMAP, and included cells with high scores for early or late IL2 signatures. Imaging analyses have shown that, even in unperturbed conditions, some Treg cells circle around IL2-producing activated Tconv cells, the balance between cytokine diffusion and capture by Tregs creating local spatial niches (21, 22). One might propose that these Tregs with high IL2 scores in control mice represent these events.

Changes in Treg Cell States. After these successive waves of transcriptional induction and repression, what state do the cells reach? First, and in keeping with previous reports (3), the presence of transcripts associated with the cell cycle among the Mid and Late signatures suggested that many of the Treg cells in treated might entered into cell division. Indeed, displaying the integrated signature of cell cycle genes on the UMAP (Fig. 4*A*) revealed their activation around 64 h, primarily in clusters 9 to 11. To determine the proportion of cells that divide during this period, we analyzed by flow cytometry the expression of Ki67, the marker of cell division, in Treg cells treated in vivo with IL2 (same mode and dose as above). This analysis (Fig. 4*B*) revealed a global shift in Ki67 staining, suggesting that a sizable fraction of the Treg population was dividing.

It has been unclear whether IL2 can achieve a maturation of rTreg into aTreg states, in the same way as TCR-driven activation can. To test this question, we computed signature scores for genes typical of rTreg and aTreg (from ref. 41). By those criteria, the

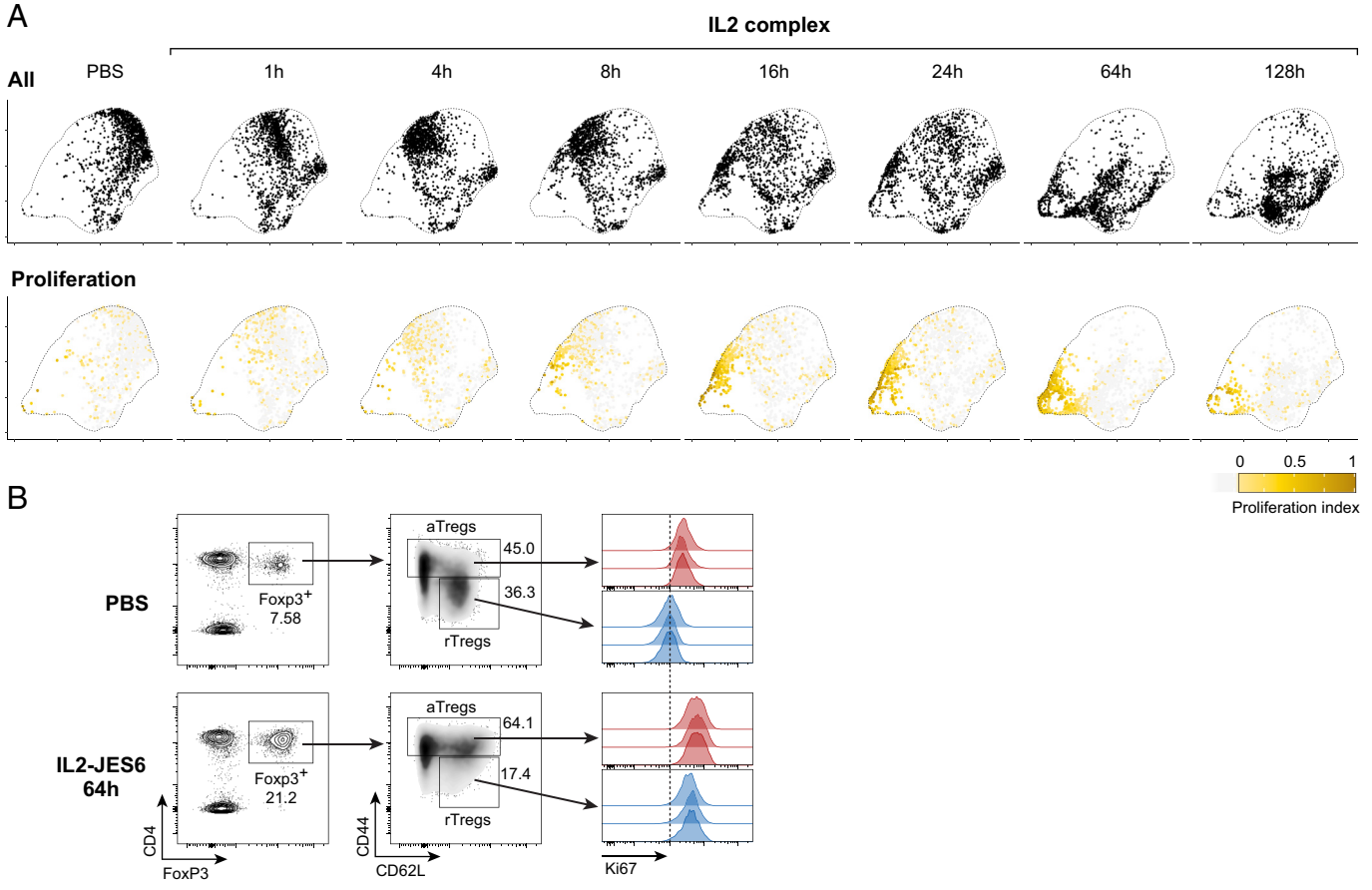

Fig. 4. IL2 stimulation induces changes in Treg cell states. (*A*) Same scRNAseq data and UMAP as in Fig. 3, showing all cells at each timepoint (top row) or color-coded by cell-cycle signature genes. (*B*) Flow cytometry plot of splenocytes from mice treated for 64 h with IL2/JES6 or PBS control, showing the proportion of Treg cells (*Left* panels) their distribution in rTregs (CD62L^{hi}CD44^{lo}) and aTregs (CD62L^{lo}CD44^{hi}) subsets (*Middle* panels), and staining for the Ki67 cell cycle marker (*Right*).

majority of cells with high rTeg/low aTreg scores did not change much during the first 24 h, but shifted significantly after 64 h, remaining in a high aTreg state at 128 h (*SI Appendix*, Fig. S2*C*). These results are consistent with the induction of CD44 observed in Fig. 4*B* Thus, it would appear that the shift to an aTreg phenotype is a late event, and one that may require a transit through cell division, but then persists in the long term.

Diversity within IL2 Response Gene Clusters. The results from Fig. 3 suggested that Tregs with different starting phenotypes vary in their responses to IL2. We then asked whether all IL2 responsive genes are induced in a synchronized manner, or whether responsive genes fall in distinct clusters that are preferentially active in different cells. A first overall representation of responsive genes, selected in Seurat as most specific of each timepoint (Fig. 5*A*), mostly revealed the general unfolding of the response with successive induction of different genesets, but no obvious subclusters. For a more resolving perspective, we analyzed the expression of all transcripts of the Early signature in all cells from the 4 h timepoint, splitting the cells as outlined in Fig. 5*B* into the main rTreg group (#1), the main aTreg group (#2), and a small group of rTregs, eccentric on the UMAP, and which seemed less responsive in Fig. 3*C* (#3). Genes were then clustered according to expression in these three groups. As expected, aTregs appeared less responsive than rTregs for genes of ClusterA and ClusterB, but cells of group 3 were the most distinctive, with a high induction of genes in ClusterA but a lower response for genes of Clusters B and C. Interestingly, ClusterA contains several transcripts typical of Treg cells (*Il2ra, Lrrc32, Gpr83*) but is otherwise entirely devoid of larger groups of genes associated with cell remodeling (ribosome biogenesis, translation, amino acid metabolism, *Myc*), all of which belong to clusters B and C. Thus, this analysis uncovers a subgroup of Treg cells that do not respond to IL2 with major cellular reprogramming, but only by modulating a few key transcripts.

We previously described the induction of many interferon signature genes (ISGs) by IL2, which we attributed to the activation of STAT1 by IL2 and several other γc cytokines (31). In the present dataset, ISGs were expressed at baseline in a small set of rTregs distinct from the main rTreg group (Fig. 5*D*); these might be similar to the small groups of ISG^{hi} T cells reported in several studies (43, 44), perhaps because they reside in an Interferon-rich microenvironment. Upon IL2 treatment, we observed a rapid response, detectable after only 1 hr, and present in most rTregs. This response then waned somewhat, before a second round of induction at 24 to 64 h (Fig. 5*E*). This biphasic ISG response was mirrored by the expression of Stat1, the key transducer of responses to IFN: overexpression of *Stat1* was notable at 24 and 64 h (Fig. 5*F*). IL2, even complexed with JES6, activates NK cells and CD4+ T cells (31) to release interferon. We propose that the immediate response is due to cell-autonomous activation of STAT1 by IL2 in Tregs, but that the later and more sustained induction of ISGs may be indirect.

Stat5 and Stat1 are both connected to the IL2 receptor, but it is unclear if they are equally involved in the context of a full activation by IL2. It was thus of interest to ask whether the responses of IL2-induced and of ISG signatures were correlated upon IL2 administration. To this end, we compared the Early-induced and ISG signature scores for each cell at different timepoints. In PBS-treated controls, cells with high ISG and IL2 signatures were wholly distinct (Fig. 5 *G*, *Left* panel). This dichotomy may reflect spatial segregation, each "tail" in the plot encompassing Tregs present in small IL2- or IFN-high compartments at baseline. At short times after IL2 injection, the ISG score increased in most cells, with little relationship between the ISG and IL2 induction scores: Cells with highest ISG score had middling IL2 scores, and cells with the highest IL2 induction score had low ISG scores (Fig. 5 *G*, *Mid* panel), which suggests that the relative contribution of Stat1 and Stat5 to IL2 signaling is not equivalent between cells.

scATACseq: Different Responses to IL2 in rTreg and aTregs. Having established the heterogeneity in transcriptional activity of Treg cells exposed to IL2, it was of interest to assess how these changes were reflected in the underlying chromatin structure. We generated scATAC-seq profiles of splenic Tregs from mice treated acutely with IL2 or PBS control as above (2 h). This short exposure led to a marked shift in Treg chromatin states (Fig. 6*A*). After classifying cells as rTreg and aTregs based on relative accessibility of specific OCRs (17), the UMAP visualization (Fig. 6*B*) showed that rTreg populations shifted more than did aTreg cells in response to IL2 (median Local Inverse Simpson's Index (45) between treated and untreated 1.13 in rTreg vs. 1.60 in aTreg, $P < 2.2 \times 10^{-16}$). Visualization of the closest cells in treated vs. untreated pools in high-dimensional OCR space [nearest neighbor in an LSI embedding with IL2 effect removed (45)] confirmed that all rTregs responded sharply but only a fraction of aTregs did (Fig. 6*C*). A major component of the response to IL2 involves binding of some OCRs by phosphorylated STAT5 (27, 46, 47). We quantitated, for each cell, the changes in ATAC signal in OCRs that contain STAT5 motifs. While these OCRs opened strongly and homogenously in rTreg cells, their response was generally lower and more variable in aTreg cells (Fig. 6*D*). Thus, the variability in IL2-induced changes at the mRNA level (Fig. 3) were anchored in chromatin accessibility between groups of Treg cells.

Mechanistically, the lesser response of aTregs was also reflected by lower induction of STAT5 phosphorylation after exposure to IL2 in culture (Fig. 6*E*). It was explainable, at least in part, by a lower presence of the high affinity receptor trimer, identified by anti-CD25 staining, on the surface of aTregs relative to rTregs (Fig. 6*D*).

In recent work, we combined several experimental strategies with Machine Learning ("topic modeling") to quantitatively decompose the combinatorial architecture of the genetic regulatory network in Treg cells (17), The resulting framework provides a holistic and clarifying perspective on the different chromatin programs that determine both the identity and phenotypic diversification of Treg cells. Since IL2 is such a central factor for Treg identity, it was of interest to ascertain how its effects played out in this Topic framework (Fig. 6 *G* and *H*). As might be expected, no topic uniquely encompassed the response to IL2. Induced OCRs were specifically enriched for Topics 3, 4, and 12. Overlay onto the framework highlighted a specific induction of STAT-motif containing nodes. Topic 12 contains an interferon-responsive component, and its induction was consistent with the ISG component described above. Accordingly, both STAT5 and STAT1/3 families were associated with Topic 12 changes (Fig. 6*H*). Conversely, IL2 repressed RUNX and ETS motifs in Topics 5, 16, and 17 and Forkhead motifs in Topic 17. These chromatin programs are also preferentially active in Tconv, suggesting that IL2 bolsters Treg identity by suppressing Tconv-specific features, a notion of interest given IL2's role in supporting Treg differentiation (19). Thus, chromatin topics captured the specific response to IL2, described differences across cell states, and highlighted connections to different inductive and repressive mechanisms of IL2 action.

Transcription Factor Networks that Control Treg Responses to IL2. We next investigated how the Treg TF regulatory network controlled and adapted to IL2. Paired single cell transcriptomic and chromatin datasets of the same biological process can enable

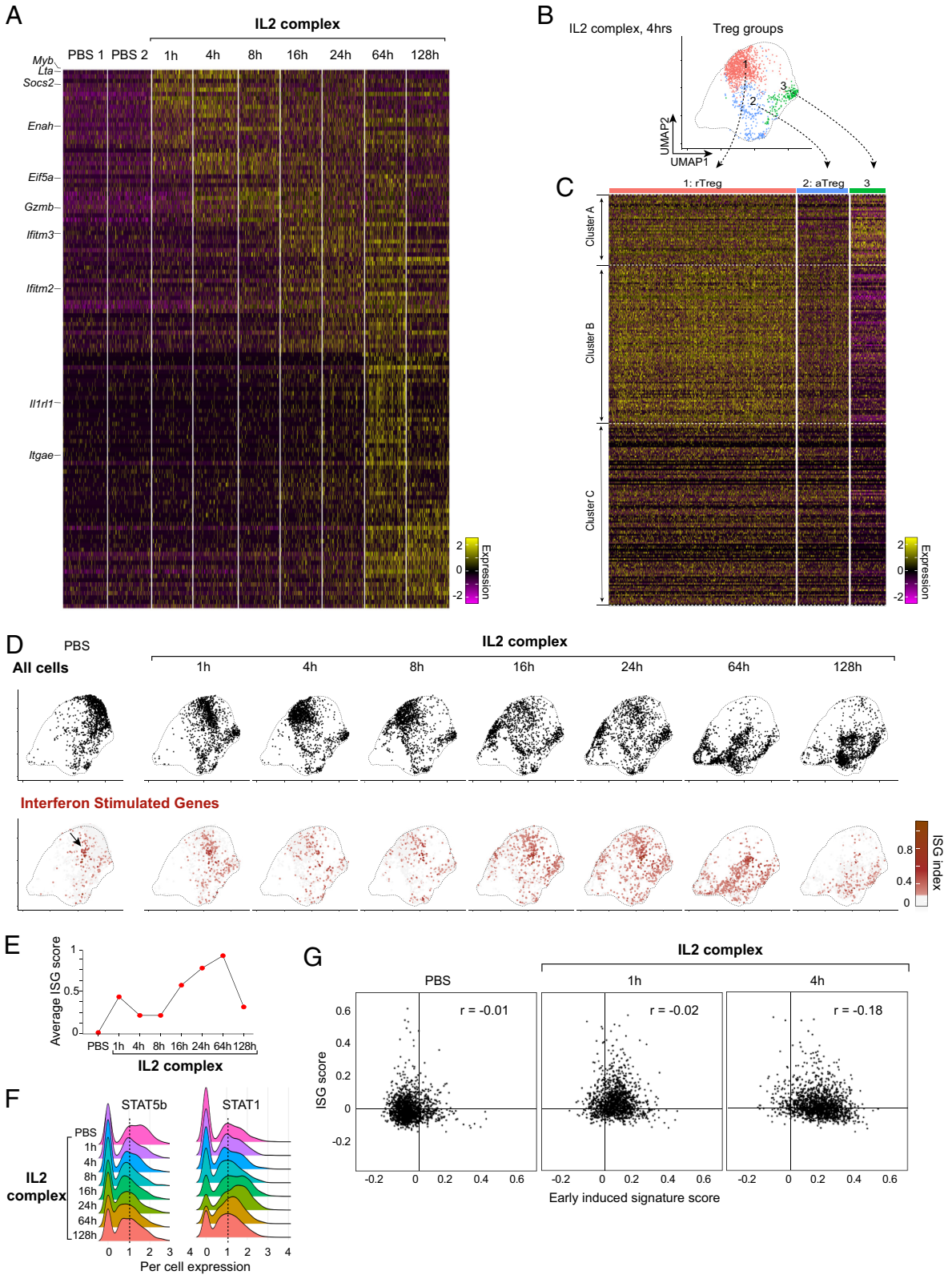

Fig. 5. Diversity within Treg responses to IL2. Same mouse treatments and scRNAseq data as in Fig. 3. (*A*) Heatmap showing top differential genes for each timepoint, selected by the FindMarkers function in Seurat. (*B*) Treg cells at the 4 h timepoint were separated into the main rTreg group (group 1), aTregs (group 2), and a group of less-responsive rTregs (group 3—also identified in Fig. 3*C*). (*C*) Heatmap of genes in the early-induced signature (from Fig. 1) clustered by k-means according to their expression in cells from groups 1, 2, and 3 (from Fig. 5*B*). (*D*) UMAP showing all cells per timepoint (*Top*) and the computed Interferon Stimulated Genes index (from ref. 42, Dataset S3). (*E*) Average ISG score over the timecourse of the response to IL2. (*F*) Expression of *Stat5b* and *Stat1* in Treg cells from control (PBS) and IL2-treated mice at the indicated timepoints. (*G*) Scatter plot comparing the early IL2-induced signature (from Fig. 1*A*) and the ISG scores for each cell in PBS, 1 h- or 4 h-stimulated Treg cells).

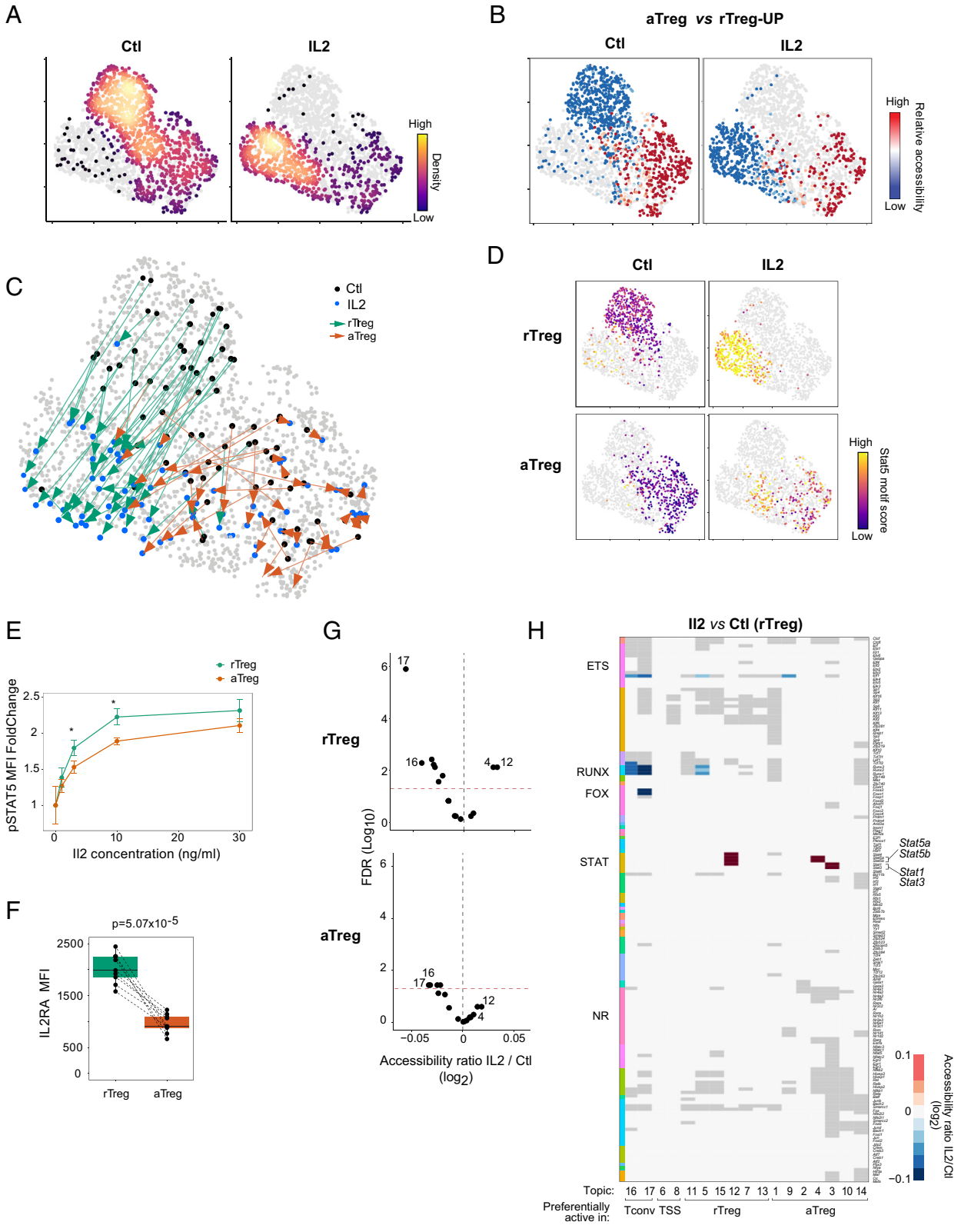

Fig. 6. Chromatin changes in response to IL2. (*A*) UMAP of scATAC-seq of splenic Tregs or PBS control for 2 h, colored by density of cells from each condition. (*B*) Relative accessibility (chromVAR scores) of OCRs increased in accessibility in aTreg vs. rTreg populations visualized on UMAP of scATAC-seq data from (*A*) and split by treatment group. (*C*) Visualization of pairs identifying the closest cells in IL2-treated and PBS conditions in high-dimensional OCR space onto UMAP from (*A*), and colored by the cell state (rTreg or aTreg) of the untreated, control cell in each pair. Random samples of 40 pairs of rTreg control and 40 pairs of aTreg control cells shown for visual clarity. (*D*) Relative accessibility of OCRs containing Stat5 motif (chromVAR scores), visualized on UMAP from *A* and split by cell state and treatment status. (*E*) Fold Change of rTreg or aTreg pSTAT5 mean fluorescence intensity, relative to untreated control, after ex vivo stimulation with indicated concentration of IL2 for 15 min. *P* values from *t* test. N = 3 mice. (*F*) IL2RA (CD25) mean fluorescence intensity among splenic rTreg or aTreg. *P* value from paired *t* test. N = 9 mice. (*G*) Differential accessibility per topic between aggregated IL2 treated vs. untreated spleen Treg scATAC profiles, separated by cell state. (*H*) Differential accessibility per motif in each topic (FDR < 0.05) between IL2-treated and untreated control rTreg overlaid onto motif to topic connections (enrichment only-version of network) from ref. 17. Gray indicates significant topic motif enrichment from analysis in ref. 17 but no significant change in accessibility across treated vs. untreated comparisons.

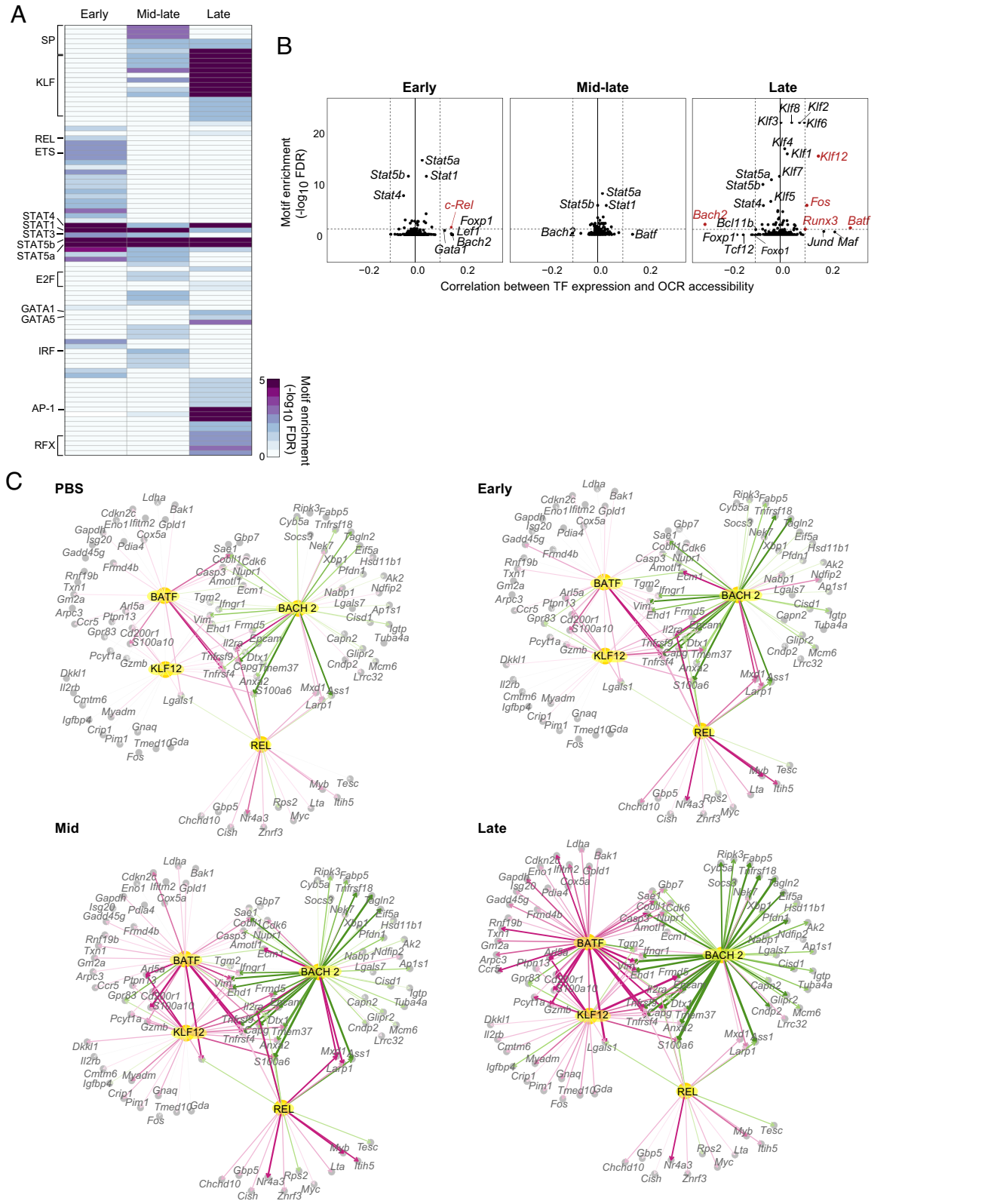

Fig. 7. Mapping the transcription factor networks that control Treg responses to IL2. (*A*) Heatmap showing the motif enrichment (−log10 FDR, permutation test) of the indicated transcription factor (TF) motifs in OCRs linked to gene sets induced at early, mid-late, and late timepoints. (*B*) The correlation (x-axis) between TF expression and accessibility of target OCRs which contain the cognate TF motif and are linked to genes from the indicated gene sets (computed in the cells from the relevant time point for each gene set) vs. gene set motif enrichment (y-axis, −log10 FDR as in *A*). Transcription factors highlighted in red indicate |correlation| > 0.1 (with permutation FDR < 0.05) and motif enrichment FDR < 0.10. (*C*) TF-gene expression correlation network of major TFs from *B* across different timepoints. Positive correlations in pink, negative correlations in green.

reconstruction of underlying gene regulatory networks. To gain temporal resolution on chromatin changes in response to IL2, we generated another scATAC-seq data of Tregs from Foxp3-GFP reporter mice treated with mIL2/JES6 complexes (10/100 μg) at the same time points as for the scRNA-seq data, hashtagged into one large dataset. Unfortunately, a technical failure in the

hashtag library of this large experiment made the demultiplexing impossible. We used a computational strategy to pair cells from the scRNA-seq and scATAC-seq datasets (48), with label transfer (49) to identify cells in the scATAC-seq dataset corresponding to the different time periods (pre, early, mid and late) in the scRNA-seq data (*SI Appendix*, Fig. S2*A*). As validation of this approach, the chromatin signature of our prior 2 h IL2 stimulation experiment was induced most highly specifically in cells assigned to the earliest timepoints (*SI Appendix*, Fig. S3*B*).

We leveraged these scRNA–scATAC pairings to learn regulatory relationships underlying the IL2 response. To identify candidate *cis*-regulatory elements relevant to the IL2 response, we computed correlations between the expression of each gene and the accessibility of its nearby OCRs (Dataset S4). We then linked these OCRs to TFs whose motifs were statistically enriched among OCRs significantly connected to genes from each of the IL2-induced gene sets from Fig. 1 (Dataset S5*A*). We focused on the induced gene sets as the repressed gene sets had few significant motif enrichments (Fig. 7*A* and *SI Appendix*, Fig. S3*C*). Underscoring their dominant contribution to the IL2 response, STAT motifs were enriched among OCRs linked to gene sets from all three timepoints (Fig. 7*A*). Other motif families had more restricted patterns. OCRs linked to the Early signature genes were enriched in ETS and REL motifs, while KLF/SP motifs were enriched in the mid-late induced group and even more strongly in the late induced gene set, and AP/1 and RFX motifs were enriched in the late induced genes. IRF and E2F motifs were enriched in the mid-late induced group, echoing the induction of ISGs and proliferation signatures, respectively. Thus, paired scRNA and scATAC data linked TFs to induction of different groups of IL2-responsive genes.

While motif enrichment can nominate families of TFs, narrowing in on individual TFs requires orthogonal data to overcome within-family motif similarity. Expression values for the individual factors in the scRNA-seq data provide one such opportunity. To nominate TFs modulating *cis*-regulatory activity at IL2-relevant loci, we calculated the correlation of each TF's expression vs. the accessibility of OCRs which contained its cognate motif, and which had significant links to genes from IL2-responsive gene sets. Plotting this correlation vs. the motif enrichment score (Fig. 7*B* and Dataset S5*B*) distinguishes two modes of association; opening at OCRs connected to Early induced genes were most correlated with expression of the NF-kB member cRel (Fig. 7 *B*, *Left* panel). In contrast, TFs like Stat5a and Stat5b show stronger motif enrichment, but no correlation, because their activity is not regulated by increased expression but by posttranslational modification (Fig. 5*F*).

Genes induced later in the response were positively associated with multiple AP-1 TFs (e.g., Batf, Fos) and Runx3, consistent with prior findings (32) and multiple KLF members, of which only KLF12 was both significantly enriched and correlated. Maf family members have been previously identified as differentially expressed in the response to IL2 (3)—in our network, which leveraged both chromatin and expression data, Maf was significantly correlated but not enriched in the late-induced genes, suggesting it is a secondary contributor to the IL2 response. Bach2 was a prominent putative negative regulator. Importantly, Bach2 switched from being a positive regulator for earlier induced genes to a negative one later in the response, suggesting dynamic changes in its regulatory activity and a negative feedback mechanism (accordingly, Bach2 is down-regulated at late times of the response—Dataset S1). Batf had significant positive and Bach2 had significant negative association with the late induced gene OCRs even in the PBS condition, consistent with the IL2-signaling in control mice described in Fig. 3, but all correlations increased upon IL2 stimulation (Fig. 7*B* and *SI Appendix*, Fig. S3*D* and Dataset S5*C*). Thus, TF correlation analyses homed in on specific TFs controlling the IL2 response and parsed their temporal effects.

Finally, we used the top TFs nominated from this analysis to generate a TF-gene regulatory network (Fig. 6*C* and *SI Appendix*, Fig. S4*A*). We constructed this network from gene–gene correlations of TFs and genes from each of the induced gene sets across individual cells in the scRNAseq data (analytical power here derives from the coordinated responses to IL2 but also from the cell-to-cell fluctuations across the dataset; Dataset S6*A*). We retained only significant TF-gene connections (permutation test) where OCRs linked to each gene also contained the corresponding TF motif. Each time point showed progressively greater number and strength of regulatory connections compared to the PBS control. At the earliest timepoint, initial induction above PBS was strongest through Rel-associated OCRs (including *Myb* and *Myc*), with weaker links to Batf and Klf12. Bach2 had both positive and negative connections to different genes. Progression of the response was marked by decreasing association with Rel and increasing association with Klf12 and Batf-linked genes. Importantly, Klf12 itself induced Batf and Fos, suggesting it functions at the top of the hierarchy of TFs in the later part of the response. Bach2 also became a primarily negative regulator, consistent with Fig. 7*B*. Batf, Bach2, and Rel all positively contributed to *Il2ra* expression, and KLF12 positively controlled *Il2rb*, explaining a positive feedback loop of IL2 sensing. Note, as mentioned above, that these gene–gene correlations between TF and target will miss effects mediated at the protein modification level, which is why STAT5 does not appear in the networks of Fig. 7*C*. We thus separately generated a network based on correlation of accessibility of TF target OCRs and the expression of their linked genes, also including the significantly enriched STAT motifs in the analysis (*SI Appendix*, Fig. S3 and Dataset S6*B*). Here, Stat5 factors dominated the network (including associations with *Il2ra* and *Il2rb*), and this analysis again showed a progression from Rel- and Runx3-linked genes to increasing control of Klf12 and AP-1 factors (Fos and Batf). Consistent with prior reports of Gata1 inactivation contributing to regulation of middle time points (32), STAT motifs negatively regulated *Gata1* expression in this network. Thus, the refined regulatory network identified the individual gene targets of the major TF controllers of the IL2 response in Tregs.

Discussion

This study shows the Treg response to IL2 as a coordinated, yet heterogenous, rewiring that is more nuanced and complex than a binary "on/off" switch. Using a broad time course of stimulation, from 1 to 128 h, the data fully captured the changes in transcriptional and epigenomic programs that unfold over time of stimulation, but also point to diversity in the responses: There is not true equity in how different Treg cells respond, and different gene modules are not equally included across all Treg subsets.

Tregs mount a very rapid and coherent transcriptional and chromatin response to IL2, which we found to be already maximal, in terms of the number of responding genes, by 4 h after treatment. These results differed in this respect from a previous study, which reported a slower and more accumulative course (32). We suspect that the difference may be due to the doses administered, or to the statistical threshold used for gene counting. Importantly, however, the response clearly morphed over time, as evidenced by the evolving signatures (Fig. 1), the cell trajectory across the multidimensional UMAP space (Fig. 3), and by the changing impact of specific transcription factors (Fig. 7). These changes included the activation of canonical pathways described in previous studies (31, 32, 50) that denote IL2's profound reworking of cell states, including Myc and

other mTOR-associated metabolic transcripts. These transcriptional shifts were mirrored at the chromatin level, with widespread opening of STAT5-bound regions and a broad remodeling of accessible chromatin. This rapid response points to a "poised" state in many Tregs, ready to respond to IL2-mediated cues, from high expression of CD25 and intracellular signaling machinery geared toward an immediate response to fluctuating IL2 levels.

The scRNAseq data also highlighted a small group of Treg cells which display high IL2 signature scores at steady state in unperturbed mice (Fig. 3*A*). These included Tregs in which either early or late IL2 signatures predominated, implying that the whole cycle of the Treg response to IL2 operates continuously on some Tregs at baseline, likely driven by sporadic Tconv activation by environmental antigens. It may be worth nothing that the acute CD25 knockout rapidly affected large proportions of rTregs (50), more than the few percent found here with a high IL2 signature score in control mice. Thus, IL2 probably operates at two levels at baseline: a small proportion of Treg cells with high exposure that drives a full response, and a lower but more widespread level of exposure that supports the maintenance of the Treg pool.

The fine analyses of the single-cell data reported here also highlight strong disparities in the ability of different Treg subsets to respond to IL2. At both the chromatin and transcriptional levels, aTregs presented a weaker and more variegated response, even under saturating doses of the cytokine doses. This disparity between rTreg and aTreg is consistent with prior observations (50, 51). Smigiel et al. previously reported a low responsiveness to IL2 in $CD44^{hi}CCR7^{lo}$ Tregs (51), interestingly attributing it to an inability of those cells to use CCR7 to home to locales of high IL2 concentration. Since the injected IL2/JES6 complexes in our experiments are diffusible and not constrained by local production, the present results probably negate this interpretation. Instead, they indicate an intrinsically low response of aTregs to IL2 relative to rTregs, that involves, in a cell-autonomous manner, all players (receptor, STAT, chromatin) in the Treg response to IL2: aTregs express less CD25, exhibit less STAT5 phosphorylation upon IL2 exposure, and show weaker accessibility changes in STAT5 motif-containing regions. These results are congruent with the relative insensitivity of aTregs to acute CD25 ablation, which might have been attributed to compensating homeostatic expansion that pushes Tregs into an aTreg state (52). Together, they suggest a shift toward other homeostatic regulators. There is certainly the precedent of ST2+ aTreg cells that are driven by IL33 (53, 54, 55), but our results suggest a wider shift, which might be worth exploring since aTregs represent the primary effector state for Tregs.

The diversity in Treg responses to IL2 extends beyond the rTreg/aTreg dichotomy: A small group of rTreg cells with high CD25 expression (cluster 3 in Fig. 5) seem to eschew the broad cell activation response (ribogenesis, activation of transcription, and translation) driven by IL2 and Myc in most Tregs, and instead only induce a smaller subset of responding genes, several of which are typical Treg genes. Overall, these results hint at a more modular IL2 response architecture, where certain functional modules (e.g., suppressive capacity) can be uncoupled from others (e.g., proliferation, metabolism). This concept could have significant implications for designing IL2-based therapeutics that aim to boost regulatory function without necessarily expanding the Treg pool.

Even more heterogeneity was detected in the activation of ISGs by IL2. It was biphasic: first, a very fast response (1 to 2 h) which we attribute to a cell-autonomous activation of STAT1 by IL2 (1, 3), which was followed by a delayed wave that might reflect interferon released by NK and Tconv cells in response to IL2. But it was clear that these responses were again not uniform, even among rTreg cells, especially at early times (Fig. 5*D*). Indeed, the divergence between the induction of ISGs and of IL2-early signatures at the early timepoints (Fig. 5*G*) suggested that individual cells vary in the degree of Stat1 vs. Stat5 signaling, perhaps by variable recruitment of Stat proteins at the IL2R/JAK complex.

Finally, these results carry translational implications. Several IL2-based immunotherapies (low-dose IL2, IL2 muteins, immunocytokines, etc.) are already in clinical development (23). Our data show that rTregs are the most readily transcriptionally reprogrammable targets of such treatments, but also that Tregs exposed to IL2 do eventually adopt an aTreg phenotype (Fig. 4), with the induction of several effector molecules (Fig. 1). In addition, the results of Fig. 2 indicate that although biasing IL2 toward activation of either the trimeric or dimeric IL2 receptor successfully skews its activities toward Tregs or NK cells, respectively, effects at the genome level are still present on both cell types. It is thus important to consider the response to IL2-based interventions on both targeted and untargeted cells.

In conclusion, IL2 is not a monolithic "go" signal for Treg cells but instead a temporal and context-dependent sculptor of identity and function.

Materials and Methods

Mice and Treatments. *Foxp3*$^{ires\text{-}gfp}$/B6 (56) mice on the B6 background (bred in our colony), and C57Bl6J (Jackson) were used at 6 to 8 wk of age, under HMS IACUC IS00001257. IL2/JES6-1 complexes were administered i.v. as described (31), at 10 μg IL2 to 100 μg JES6-1. For immunocytokines (purified as described (37–39), 10 μg doses (equivalent to ~5 μg IL2) were administered i.v. in 100 μL PBS.

RNA and Chromatin Profiling. For low-input population profiling, the standard ImmGen SmartSeq2 protocol was used, using 1,000 double-sorted splenic Treg cells. External gene signatures (Dataset S3) include the IL2 signature gene sets for NK cells (31), panimmunocyte ISGs (42), cell cycle signature genes (57), and aTreg/rTreg signatures (41). scRNA-seq experiments were performed on the 10× Genomics Chromium 3′ v2 platform as described (44), samples from different time points were run together with TotalSeq hashtags (BioLegend). Data were processed using CellRanger (10× Genomics) and analyzed with Seurat (10903). scATACseq on the 10× Genomics Chromium instrument (17). used hashtagged cells with a modification of ASAP-seq (40). Data were processed and analyzed as described (17) with Signac v1.14.0 (58). For comparisons across conditions, we used a common set of Treg-specific OCRs (17) Bias-corrected relative motif accessibility was calculated using chromVAR (59).

Data, Materials, and Software Availability. RNAseq and scATACseq data have been deposited in GEO (GSE297025) (60).

ACKNOWLEDGMENTS. We thank T. Malek for insightful discussions; K. Hattori, C. Araneo, I. Magill for help with mice, cell sorting, and single-cell profiling. This work was funded by grants from the NIH (R24AI072073 to the ImmGen Consortium, R01AI150686 to C.B., and R01EB029455 and R21HL170146 to J.B.S.), the Helmsley Charitable Trust and the Kenneth Rainin Foundation to J.B.S. K.C. was supported by NIGMS Grants T32GM007753 and T32GM144273 and a Harvard Stem Cell Institute MD/PhD Training Fellowship.

1. S. H. Ross, D. A. Cantrell, Signaling and function of interleukin-2 in T lymphocytes. *Annu. Rev. Immunol.* **36**, 411–433 (2018).
2. R. Spolski, P. Li, W. J. Leonard, Biology and regulation of IL-2: From molecular mechanisms to human therapy. *Nat. Rev. Immunol.* **18**, 648–659 (2018).
3. A. N. Shouse, K. M. LaPorte, T. R. Malek, Interleukin-2 signaling in the regulation of T cell biology in autoimmunity and cancer. *Immunity* **57**, 414–428 (2024).
4. S. Gillis, M. M. Ferm, W. Ou, K. A. Smith, T cell growth factor: Parameters of production and a quantitative microassay for activity. *J. Immunol.* **120**, 2027–2032 (1978).

5. D. A. Cantrell, K. A. Smith, The interleukin-2 T-cell system: A new cell growth model. *Science* **224**, 1312–1316 (1984).
6. J. D. Fontenot, J. P. Rasmussen, M. A. Gavin, A. Y. Rudensky, A function for interleukin 2 in Foxp3-expressing regulatory T cells. *Nat. Immunol.* **6**, 1142–1151 (2005).
7. R. Setoguchi, S. Hori, T. Takahashi, S. Sakaguchi, Homeostatic maintenance of natural Foxp3$^+$ CD25$^+$ CD4$^+$ regulatory T cells by interleukin (IL)-2 and induction of autoimmune disease by IL-2 neutralization. *J. Exp. Med.* **201**, 723–735 (2005).
8. S. Z. Josefowicz, L. F. Lu, A. Y. Rudensky, Regulatory T cells: Mechanisms of differentiation and function. *Annu. Rev. Immunol.* **30**, 531–564 (2012).
9. M. Panduro, C. Benoist, D. Mathis, Tissue Tregs. *Annu. Rev. Immunol.* **34**, 609–633 (2016).
10. M. Feuerer *et al.*, Genomic definition of multiple ex vivo regulatory T cell subphenotypes. *Proc. Natl. Acad. Sci. U.S.A.* **107**, 5919–5924 (2010).
11. E. Cretney, A. Kallies, S. L. Nutt, Differentiation and function of Foxp3(+) effector regulatory T cells. *Trends Immunol.* **34**, 74–80 (2013).
12. I. K. Gratz, D. J. Campbell, Organ-specific and memory treg cells: Specificity, development, function, and maintenance. *Front. Immunol.* **5**, 333 (2014).
13. D. Zemmour *et al.*, Single-cell gene expression reveals a landscape of regulatory T cell phenotypes shaped by the TCR. *Nat. Immunol.* **19**, 291–301 (2018).
14. A. R. Muñoz-Rojas, D. Mathis, Tissue regulatory T cells: Regulatory chameleons. *Nat. Rev. Immunol.* **21**, 597–611 (2021).
15. E. Cretney *et al.*, The transcription factors Blimp-1 and IRF4 jointly control the differentiation and function of effector regulatory T cells. *Nat. Immunol.* **12**, 304–311 (2011).
16. R. N. Ramirez *et al.*, Foxp3 associates with enhancer–promoter loops to regulate Treg-specific gene expression. *Sci. Immunol.* **7**, eabj9836 (2022).
17. K. Chowdhary, J. Leon, D. Mathis, C. Benoist, An integrated transcription factor framework for *Treg* identity and diversity. *Proc. Natl. Acad. Sci. U.S.A.* **121**, e2411301121 (2024).
18. M. A. Burchill *et al.*, Linked T cell receptor and cytokine signaling govern the development of the regulatory T cell repertoire. *Immunity* **28**, 112–121 (2008).
19. S. Hemmers *et al.*, IL-2 production by self-reactive CD4 thymocytes scales regulatory T cell generation in the thymus. *J. Exp. Med.* **216**, 2466–2478 (2019).
20. O. Boyman, J. Sprent, The role of interleukin-2 during homeostasis and activation of the immune system. *Nat. Rev. Immunol.* **12**, 180–190 (2012).
21. A. Oyler-Yaniv *et al.*, A tunable diffusion-consumption mechanism of cytokine propagation enables plasticity in cell-to-cell communication in the immune system. *Immunity* **46**, 609–620 (2017).
22. H. S. Wong *et al.*, A local regulatory T cell feedback circuit maintains immune homeostasis by pruning self-activated T cells. *Cell* **184**, 3981–3997 (2021).
23. V. Lykhopiy, V. Malviya, S. Humblet-Baron, S. M. Schlenner, IL-2 immunotherapy for targeting regulatory T cells in autoimmunity. *Genes Immun.* **24**, 248–262 (2023).
24. R. Hernandez, J. Poder, K. M. LaPorte, T. R. Malek, Engineering IL-2 for immunotherapy of autoimmunity and cancer. *Nat. Rev. Immunol.* **22**, 614–628 (2022).
25. Y. Feng *et al.*, Control of the inheritance of regulatory T cell identity by a *cis* element in the *Foxp3* locus. *Cell* **158**, 749–763 (2014).
26. D. A. Frank *et al.*, Interleukin 2 signaling involves the phosphorylation of stat proteins. *Proc. Natl. Acad. Sci. U.S.A.* **92**, 7779–7783 (1995).
27. S. H. Ross *et al.*, Phosphoproteomic analyses of interleukin 2 signaling reveal integrated JAK kinase-dependent and -independent networks in CD8$^+$ T cells. *Immunity* **45**, 685–700 (2016).
28. J. D. Graves *et al.*, The growth factor IL-2 activates p21ras proteins in normal human T lymphocytes. *J. Immunol.* **148**, 2417–2422 (1992).
29. P. Brennan *et al.*, Phosphatidylinositol 3-kinase couples the interleukin-2 receptor to the cell cycle regulator E2f. *Immunity.* **7**, 679–689 (1997).
30. N. M. Chapman, H. Chi, mTOR signaling, Tregs and immune modulation. *Immunotherapy* **6**, 1295–1311 (2014).
31. A. Baysoy *et al.*, The interweaved signatures of common-gamma-chain cytokines across immunologic lineages. *J. Exp. Med.* **220**, e20222052 (2023).
32. A. Moro *et al.*, Dynamic transcriptional activity and chromatin remodeling of regulatory T cells after varied duration of interleukin-2 receptor signaling. *Nat. Immunol.* **23**, 802–813 (2022).
33. A. Cui *et al.*, Dictionary of immune responses to cytokines at single-cell resolution. *Nature* **625**, 377–384 (2024).
34. M. E. Raeber *et al.*, Interleukin-2 immunotherapy reveals human regulatory T cell subsets with distinct functional and tissue-homing characteristics. *Immunity* **57**, 2232–2250 (2024).
35. J. J. Lee *et al.*, Early transcriptional effects of inflammatory cytokines reveal highly redundant cytokine networks. *J. Exp. Med.* **222**, e20241207 (2025).
36. O. Boyman *et al.*, Selective stimulation of T cell subsets with antibody-cytokine immune complexes. *Science* **311**, 1924–1927 (2006).
37. A. B. Silver *et al.*, An engineered immunocytokine with collagen affinity improves the tumor bioavailability, tolerability, and therapeutic efficacy of IL-2. *Cell Rep. Med.* **4**, 101289 (2023).
38. E. K. Leonard *et al.*, Engineered cytokine/antibody fusion proteins improve IL-2 delivery to pro-inflammatory cells and promote antitumor activity. *JCI Insight* **9**, e173469 (2024).
39. D. VanDyke *et al.*, Engineered human cytokine/antibody fusion proteins expand regulatory T cells and confer autoimmune disease protection. *Cell Rep.* **41**, 111478 (2022).
40. E. P. Mimitou *et al.*, Scalable, multimodal profiling of chromatin accessibility, gene expression and protein levels in single cells. *Nat. Biotechnol.* **39**, 1246–1258 (2021).
41. A. G. Levine, A. Arvey, W. Jin, A. Y. Rudensky, Continuous requirement for the TCR in regulatory T cell function. *Nat. Immunol.* **15**, 1070–1078 (2014).
42. S. Mostafavi *et al.*, Parsing the interferon transcriptional network and its disease associations. *Cell* **164**, 564–578 (2016).
43. C. A. Tibbitt *et al.*, Single-cell RNA sequencing of the T helper cell response to house dust mites defines a distinct gene expression signature in airway Th2 cells. *Immunity* **51**, 169–184 (2019).
44. E. Kiner *et al.*, Gut CD4$^+$ T cell phenotypes are a continuum molded by microbes, not by T_H archetypes. *Nat. Immunol.* **22**, 216–228 (2021).
45. I. Korsunsky *et al.*, Fast, sensitive and accurate integration of single-cell data with harmony. *Nat. Methods* **16**, 1289–1296 (2019).
46. R. Moriggl *et al.*, Stat5 activation is uniquely associated with cytokine signaling in peripheral T cells. *Immunity* **11**, 225–230 (1999).
47. M. A. Burchill *et al.*, IL-2 receptor beta-dependent STAT5 activation is required for the development of Foxp3+ regulatory T cells. *J. Immunol.* **178**, 280–290 (2007).
48. V. K. Kartha *et al.*, Functional inference of gene regulation using single-cell multi-omics. *Cell Genom.* **2**, 100166 (2022).
49. R. Satija *et al.*, Spatial reconstruction of single-cell gene expression data. *Nat. Biotechnol.* **33**, 495–502 (2015).
50. A. N. Shouse, A. V. Villarino, T. R. Malek, Interleukin-2 receptor signaling acts as a checkpoint that influences the distribution of regulatory T cell subsets. *iScience* **27**, 111248 (2024).
51. K. S. Smigiel *et al.*, CCR7 provides localized access to IL-2 and defines homeostatically distinct regulatory T cell subsets. *J. Exp. Med.* **211**, 121–136 (2014).
52. J. van der Veeken *et al.*, Memory of inflammation in regulatory T cells. *Cell* **166**, 977–990 (2016).
53. C. Schiering *et al.*, The alarmin IL-33 promotes regulatory T-cell function in the intestine. *Nature* **513**, 564–568 (2014).
54. D. Kolodin *et al.*, Antigen- and cytokine-driven accumulation of regulatory T cells in visceral adipose tissue of lean mice. *Cell Metab.* **21**, 543–557 (2015).
55. J. Siede *et al.*, IL-33 receptor-expressing regulatory T cells are highly activated, Th2 biased and suppress CD4 T cell proliferation through IL-10 and TGFβ release. *PLoS ONE* **11**, e0161507 (2016).
56. E. Bettelli *et al.*, Reciprocal developmental pathways for the generation of pathogenic effector TH17 and regulatory T cells. *Nature* **441**, 235–238 (2006).
57. D. Dominguez *et al.*, A high-resolution transcriptome map of cell cycle reveals novel connections between periodic genes and cancer. *Cell Res.* **26**, 946–962 (2016).
58. T. Stuart *et al.*, Single-cell chromatin state analysis with signac. *Nat. Methods* **18**, 1333–1341 (2021).
59. A. N. Schep, B. Wu, J. D. Buenrostro, W. J. Greenleaf, ChromVAR: Inferring transcription-factor-associated accessibility from single-cell epigenomic data. *Nat. Methods* **14**, 975–978 (2017).
60. K. Seddu *et al.*, Data from "Dynamics and variegation in the Treg response to Interleukin-2." https://www.ncbi.nlm.nih.gov/geo/query/acc.cgi?acc=GSE297025. Deposited 13 May 2025.

SI APPENDIX FIGURE LEGENDS

Fig. S1. Transcriptomic changes after stimulation with different doses of IL2. A. FOXP3$^{IRES\text{-}GFP}$ mice were stimulated with different doses of IL2 equivalent from 0.1ug to 10ug showing similar level of induced and repressed gene expression patterns. **B**. Plot showing the induction index for the different injected doses of IL2 equivalent.

Fig. S2. scRNAseq cluster composition across the IL2 treatment timecourse A. Table of cell frequencies (as % of total Tregs at that timepoint), in each of the Louvain clusters shown in Fig. 3A. **B.** Significance of the change in cell frequency for each cluster across the time of response, computed by a Fisher's exact on raw cell numbers (see methods), shown as –log10(FDR). **C**. rTregs and aTregs signature scores were calculated for each cell based on the signatures from Dataset S3, and shown on a scatter plot (each dot is a cell at a given timepoint).

Fig. S3. scATAC-seq of IL2 treatment timecourse A. UMAP of scATAC-seq of IL2 treatment timecourse, colored by density of cells assigned to each condition by label transfer from corresponding scRNA-seq data. **B.** Relative chromatin accessibility (chromVAR scores) of chromatin regions increased in accessibility by 2h IL2 stimulation (from Fig 6) in cells assigned to each of the indicated timepoints, as in Fig S3A. **C.** Heatmap, as in Fig 7A, showing the motif enrichment (-log10 FDR, permutation test) of the indicated transcription factor (TF) motifs in OCRs linked to gene sets induced or repressed at early, mid-late, and late timepoints. **D.** The correlation (x-axis) between TF expression and accessibility of target open chromatin regions (OCR) which contain the cognate TF motif and are linked to genes from the indicated gene sets (computed in the PBS condition) versus gene set motif enrichment (y-axis, -log10 FDR as in Fig

7A). Transcription factors highlighted in red indicate |correlation|>0.1 (with permutation FDR < 0.05) and motif enrichment FDR < 0.10.

Fig. S4. Alternative motif-centered IL2 regulatory network. Network based on correlation between accessibility of TF target OCRs and the expression of their linked genes across cells from the indicated timepoints. Positive correlations in pink, negative correlations in green.

Fig. S1

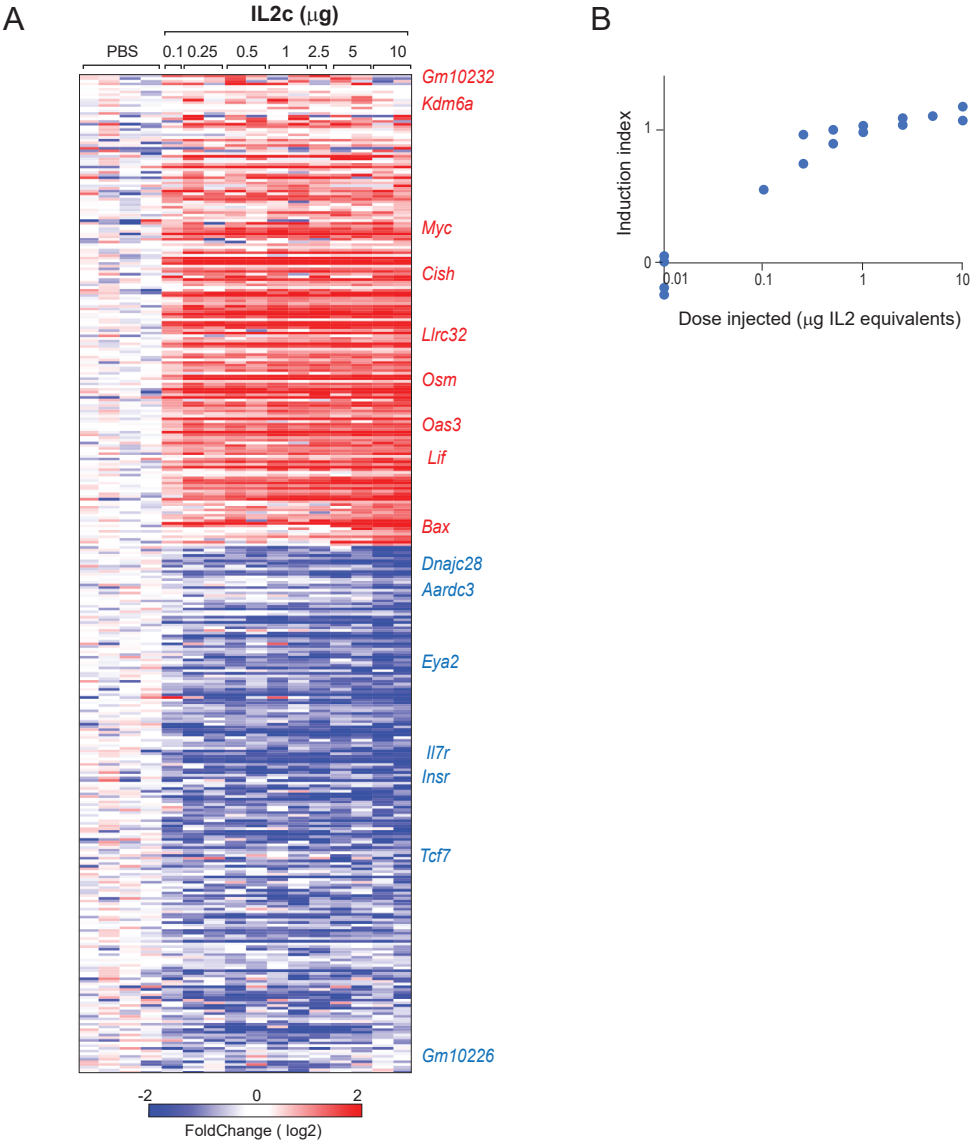
A
IL2c (μg)
PBS
0.1
0.25
0.5
1
2.5
5
10
Gm10232
Kdm6a
Myc
Cish
Llrc32
Osm
Oas3
Lif
Bax
Dnajc28
Aardc3
Eya2
Il7r
Insr
Tcf7
Gm10226
-2
0
2
FoldChange (log2)
B
Induction index
1
0
0.01
0.1
1
10
Dose injected (μg IL2 equivalents)

Figure S2

A **Fraction of cells in each cluster**

			IL2 complex						
Cluster	PBS	PBS	1h	4h	8h	16h	24h	64h	128h
0	3.91	2.52	15.79	59.25	51.78	16.91	10.24	0.85	0.87
1	14.84	13.45	15.01	12.64	11.6	13.63	16.56	13.04	17.93
2	14.39	24.52	18.2	11.28	13.21	18.17	15.12	2.75	5.37
3	54.17	47.51	5.03	1.35	1.89	2.66	3.16	0.49	2.69
4	6.18	3.31	36.83	6.64	7.13	16.28	20.41	5.64	3.63
5	0.2	0.53	0.28	0.32	0.98	0.98	2.13	38.05	58.56
6	0.13	0.13	0.28	1.1	6.57	21.59	20.62	12.26	3.49
7	1.82	3.58	3.33	3.68	3.91	4.47	4.05	1.34	1.41
8	1.82	2.32	3.26	2.32	2.17	2.73	3.37	3.45	0.94
9	0.2	0.07	0.07	0.13	0.07	0.28	0.96	12.68	2.62
10	0	0.46	0.64	0.19	0	0.7	2.54	9.09	1.61
11	2.34	1.59	1.27	1.1	0.7	1.61	0.82	0.35	0.87

B

	IL2 complex						
Cluster	1h	4h	8h	16h	24h	64h	128h
0	46.0	100.0	100.0	52.4	19.3	6.0	6.1
1	0.3	0.7	1.5	0.2	1.3	0.4	2.6
2	0.4	11.6	6.2	0.4	3.0	60.9	39.7
3	230.1	100.0	286.3	271.4	265.7	100.0	279.1
4	159.3	1.8	2.5	34.1	55.1	0.6	0.9
5	0.1	0.0	1.6	1.6	7.0	283.2	100.0
6	0.5	4.6	41.0	155.1	148.3	82.2	20.0
7	0.5	1.0	1.3	2.3	1.6	2.1	2.0
8	1.5	0.2	0.1	0.6	1.8	1.9	2.1
9	0.0	0.0	0.0	0.5	3.7	85.3	14.1
10	1.1	0.0	0.9	1.3	11.4	55.2	6.0
11	0.8	1.4	2.6	0.3	2.2	4.9	2.0

C

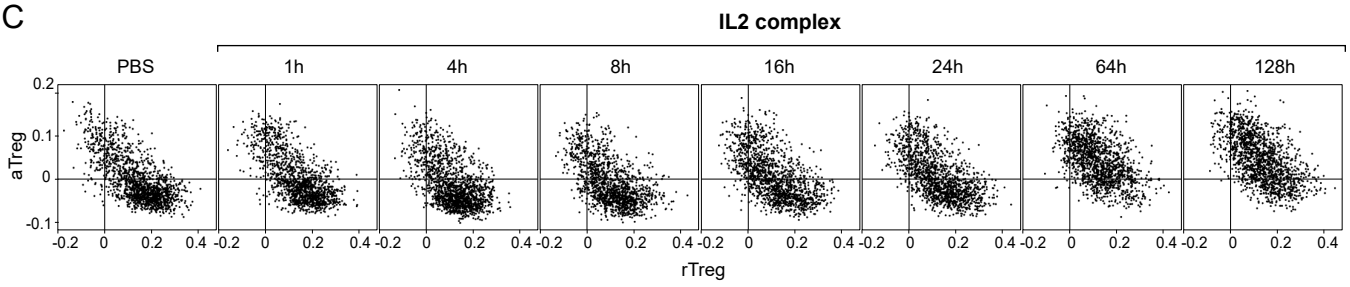

Figure S3

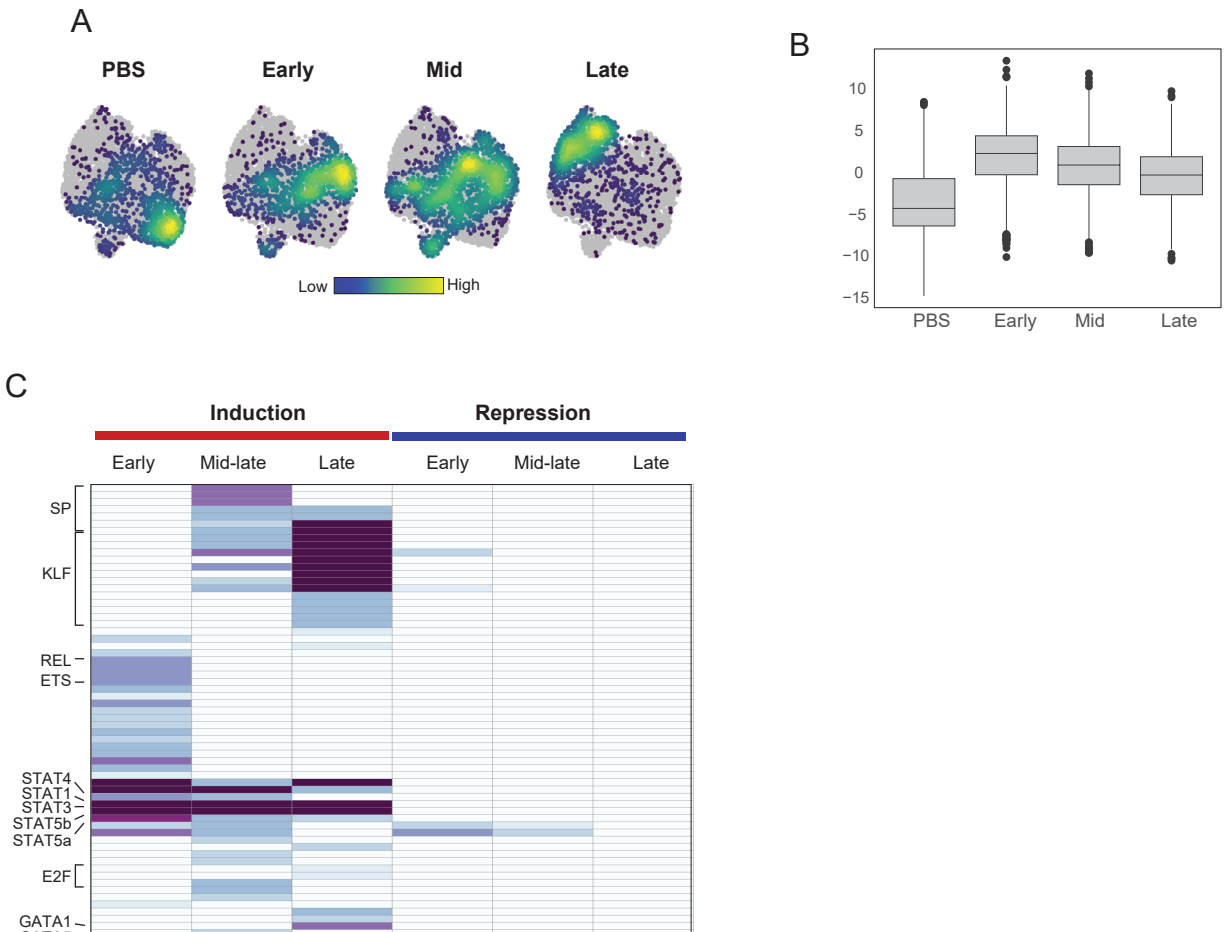
A
PBS
Early
Mid
Late
Low
High
B
10
5
0
−5
−10
−15
PBS
Early
Mid
Late
C
Induction
Repression
Early
Mid-late
Late
Early
Mid-late
Late
SP
KLF
REL
ETS
STAT4
STAT1
STAT3
STAT5b
STAT5a
E2F
GATA1
GATA5
IRF
AP-1
RFX
D
Early
Mid−late
Late
Motif enrichment (-log10 FDR)
20
10
0
Stat5a
Stat5b
Stat1
Stat4
Gata1
Rel
Foxp1
Lef1
Bach2
Batf
Klf3
Klf6
Klf2
Klf8
Klf4
Klf1
Klf12
Klf7
Stat5a
Stat5b
Fos
Klf5
Stat4
Bach2
Jund
Runx3
Batf
Foxp1
Maf
Tcf12
Bcl11b
Foxo1
−0.2
0.0
0.2
Correlation in PBS-treated cells

Figure S4

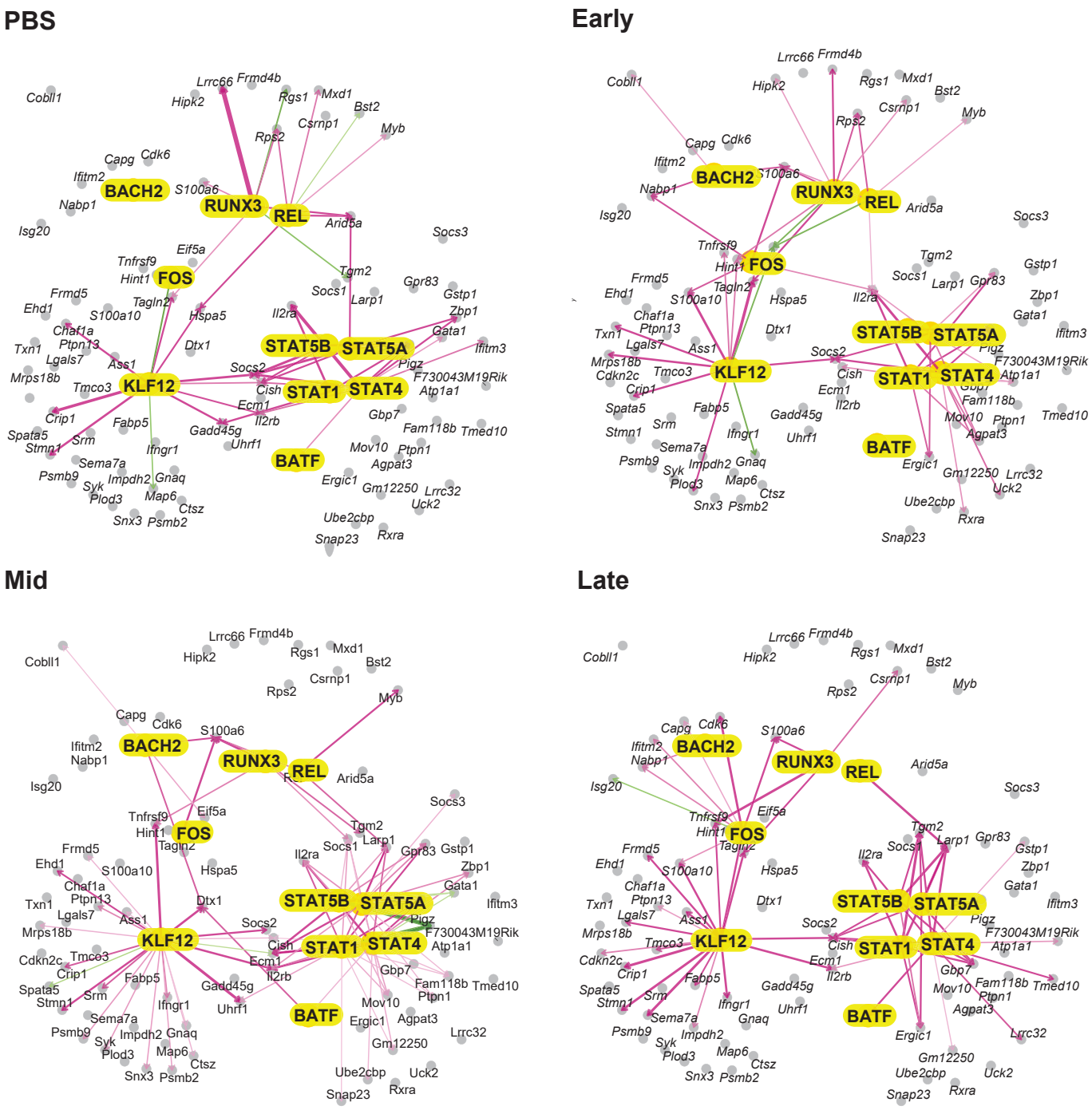
PBS
Early
Mid
Late
BACH2
RUNX3
REL
FOS
KLF12
STAT5B
STAT5A
STAT1
STAT4
BATF
Cobll1
Hipk2
Lrrc66
Frmd4b
Rgs1
Mxd1
Bst2
Csrnp1
Myb
Rps2
Capg
Cdk6
Ifitm2
Nabp1
S100a6
Arid5a
Isg20
Socs3
Tnfrsf9
Eif5a
Hint1
Tgm2
Socs1
Larp1
Gpr83
Gstp1
Zbp1
Frmd5
Ehd1
Tagln2
S100a10
Hspa5
Il2ra
Gata1
Chaf1a
Txn1
Ptpn13
Dtx1
Ifitm3
Lgals7
Ass1
Socs2
Pigz
Mrps18b
Tmco3
F730043M19Rik
Cish
Atp1a1
Ecm1
Crip1
Il2rb
Fabp5
Gbp7
Spata5
Srm
Gadd45g
Fam118b
Tmed10
Stmn1
Ifngr1
Uhrf1
Mov10
Ptpn1
Sema7a
Agpat3
Psmb9
Syk
Impdh2
Gnaq
Ergic1
Gm12250
Lrrc32
Plod3
Map6
Uck2
Ctsz
Snx3
Psmb2
Ube2cbp
Rxra
Snap23

SI APPENDIX DATASET LEGENDS

Dataset S1: Summary of IL2-induced changes over time (population RNAseq data).

Dataset S2: Summary of changes induced by Immunocytokine directed IL2 activation between cell types.

Dataset S3: Transcriptional signatures used in this study.

Dataset S4: OCR to Gene Links.

Dataset S5: (A) Gene set motif enrichment, corresponds to Fig 7A, S3C. **(B)** Source data for volcano plots in Fig 7B.

Dataset S6: **(A)** IL2 TF Regulatory Network (Gene-Gene Correlation), corresponds to Fig 7C. **(B)** IL2 TF Regulatory Network (TF target OCR accessibility-Gene Expression Correlation), corresponds to Fig S4.